ERJ Express. Published on January 28, 2010 as doi: 10.1183/09031936.00160209

MEK MODULATES FORCE FLUCTUATION-INDUCED RELENGTHENING OF CANINE TRACHEAL SMOOTH MUSCLE

Maria L. Dowell[1,2], Tera L. Lavoie[1], Oren J. Lakser[2], Nickolai O. Dulin[1], Jeffrey J. Fredberg[3], William T. Gerthoffer[4], Chun Y. Seow[5], Richard W. Mitchell[1,*], and Julian Solway[1,2,*]

Departments of [1]Medicine and [2]Pediatrics, Section of Pulmonary and Critical Care Medicine, The University of Chicago, Chicago, IL 60637; [3]Physiology Program, Harvard School of Public Health, Boston, MA; [4]Department of Biochemistry and Molecular Biology, University of South Alabama, Mobile, AL; [5]Department of Pathology and Laboratory Medicine, University of British Columbia, Vancouver, BC, Canada, V6Z 1Y6

Running head: MEK and modulation of airway smooth muscle

Supported by: NIH Grants HL 79368, AI 56352 and HD 043387

*R.W. Mitchell and J. Solway contributed equally to this work.

Corresponding author:

Maria L. Dowell, MD
Section of Pulmonary Medicine
Department of Pediatrics
The University of Chicago
5841 S. Maryland Avenue, MC4064
Chicago, IL 60637
Fax: 773-834-1444
E-mail: mdowell@peds.bsd.uchicago.edu

ABSTRACT

Tidal breathing, and especially deep breathing, is known to antagonize bronchoconstriction caused by airway smooth muscle (ASM) contraction; however, this bronchoprotective effect of breathing is impaired in asthma. In vitro, force fluctuations applied to contracted ASM cause it to relengthen – force fluctuation-induced relengthening (FFIR). Given that breathing generates similar force fluctuations in ASM, FFIR represents a likely mechanism by which breathing antagonizes bronchoconstriction. Thus, it is of considerable interest to understand what modulates FFIR and how ASM might be manipulated to exploit this phenomenon.

We demonstrated previously that p38 MAPK signaling regulates FFIR in ASM strips. Here we hypothesize that the MAPK kinase (MEK) signaling pathway also modulates FFIR. To test this hypothesis, we measured changes in FFIR in ASM treated with the MEK inhibitor, U0126.

Increasing concentrations of U0126 caused greater FFIR. U0126 reduced ERK1/2 phosphorylation without affecting isotonic shortening or MLC_{20} and p38 MAPK phosphorylation. However, increasing concentrations of U0126 progressively blunted phosphorylation of h-caldesmon, a downstream target of MEK. Thus, changes in FFIR exhibited significant negative correlation with h-caldesmon phosphorylation.

Our data demonstrate FFIR is regulated through MEK signaling and suggest the role of MEK is mediated in part through caldesmon.

Key words: asthma, airway smooth muscle, bronchoconstriction, smooth muscle mechanics, tidal breathing

INTRODUCTION

Bronchoconstriction and airflow obstruction during an asthma attack is in part a result of excessive contraction of airway smooth muscle (ASM). The extent of airway narrowing during bronchial provocation is not predicted solely, or even principally, by the ability of ASM to generate isometric force (1-10). In animals and normal human individuals subjected to bronchial provocation, airway constriction is dramatically attenuated by tidal breathing (9, 11-13) and deep inspirations, which are among the most potent of all known bronchodilatory interventions (10, 14). These results probably arise because during breathing, force fluctuations transmitted from lung parenchyma act directly on contracted ASM to influence its ability to maintain a shortened state; as a result, airway caliber becomes equilibrated dynamically (3, 4, 8) at a length longer than that in static state.

In isolated bovine ASM that is contracted isotonically, initiation of force fluctuations causes appreciable muscle relengthening (4, 15). We have demonstrated that such force fluctuation-induced relengthening (FFIR) is physiologically regulated (15, 16). For example, pharmacological inhibition of p38 mitogen-activated protein kinase (MAPK) activity, a signaling kinase known to modulate smooth muscle contraction (17), also potentiates FFIR in bovine tracheal smooth muscle (TSM) strips (15). Because mitogen-activated protein kinase kinase (MEK) has also been implicated in regulating smooth muscle contraction (18-20), we hypothesized that MEK signaling might also affect FFIR.

Acetylcholine (ACh) activation of G-protein-coupled muscarinic receptors (21) results in the initiation of several signaling cascades. Activation of myosin light chain (MLC) kinase and

MEK promote MLC_{20} phosphorylation via elevated intracellular calcium and ras signaling, respectively. Also the ras/Raf/MEK signaling cascade activates (phosphorylates) extracellular signal-regulated kinases (ERK) 1/2 and its downstream regulators of contraction such as integrin-linked kinase (22, 23) and caldesmon (24-27).

In the present study, we test the hypothesis that the MEK signaling pathway regulates FFIR in TSM using an inhibitor of MEK, U0126. We found that during MEK inhibition, changes in FFIR correlated inversely with caldesmon phosphorylation. In contrast, MEK inhibition neither reduced MLC_{20}, p38 MAPK, and heat shock protein (HSP)27 phosphorylation, nor did it reduce isotonic shortening. These results demonstrate that MEK is a key regulator of FFIR, and suggests that its effect, at least in part, is mediated through caldesmon phosphorylation.

METHODS

Tissue preparation. In accordance with IACUC approved protocols, dogs were anesthetized and euthanized by an overdose with pentobarbital sodium (30 mg/kg iv). Tracheas were removed and rinsed in Krebs-Henseleit (K-H) solution containing 115 mM NaCl, 25 mM $NaCO_3$, 1.38 mM KH_2PO_4, 2.51 mM KCl, 2.46 mM $MgCl_2$, 2.5 mM $CaCl_2$, and 11.2 mM dextrose. K-H was gassed with 95% O_2/5% CO_2 to maintain a pH between 7.3 and 7.5 and all studies were conducted at 37ºC in K-H solution. Some tissues were stored for up to 4 days at 4ºC prior to study, without apparent effect on results.

As described previously (16), parallel fibered bundles of TSM measuring 0.25-0.5 mm in width and 0.5-1.0 mm in depth were dissected free of overlying connective tissue and epithelium. Each

muscle strip was attached at either end in aluminum foil clips (Laser Services Inc., Westford, MA) that held the muscle firmly. One clip was slipped over a rigidly held hook at one end of a horizontal dip-tray style of organ bath. The other clip was fastened to a hook connected to a 300B lever arm/force transducer (Aurora Scientific, Aurora, Canada) that measured both force output and length changes, which were monitored using ADInstruments Powerlab Chart software.

Tissue equilibration. Over approximately 90 minutes, tissues were contracted periodically (~10 - 15 min intervals) using 43 mM KCl-substituted K-H solution to establish reference length (Lref). Lref measured between 3.5 and 8.0 mm. Resting length was adjusted between responses until developed force was maximal and repeatable. As previously shown, this concentration of KCl is optimal for canine TSM voltage-dependent contraction and does not cause release of ACh from neural elements in the tissue preparation (28).

Isometric protocols. After equilibration, TSM strips were exposed for at least 45 minutes to U0126 (15 or 30 μM) or vehicle, then cumulative ACh concentration-response studies were performed (10^{-9} M to 10^{-4} M). All isometric data in response to ACh were normalized to the contraction elicited during the last exposure of each muscle to 43 mM KCl-substituted K-H.

FFIR protocols. After equilibration, tissues were isometrically contracted by switching perfusion solution to K-H solution containing 10^{-4} M ACh and maximal response was noted (Fmax). Muscles were allowed to relax by reperfusing with K-H alone. Lref and Fmax were then used as base parameters for force oscillation protocols described below (Figure 1A). Twenty minutes after force reached relaxed baseline, tissues were re-exposed to 10^{-4} M ACh, and

allowed to shorten isotonically against an afterload of 32% Fmax for 20 min. During continued ACh exposure, sinusoidal force oscillations (to simulate tidal breathing) were then superimposed (0.2 Hz and amplitude ± 16% Fmax) for 20 min (4, 15, 16, 29). FFIR was noted at the end of 20 min and ACh was washed out. Muscles were oscillated using Aurora Scientific Dynamic Muscle Control (DMC) software. Muscle force and length outputs were acquired through a National Instruments PCI-6036E data acquisition board (Austin, TX); data were monitored and collected using both LabView-based DMC and ADInstruments PowerLab Chart software (Colorado Springs, CO). Next, tissues were incubated for 1 hr in K-H solution containing 3, 15, or 30 μM U0126 (Promega, Madison, WI), or 0.03% DMSO (vehicle control). Prior studies had shown that this concentration of DMSO did not affect subsequent length changes for the isotonic/force oscillation protocol (16). These concentrations of MEK inhibitor were chosen based on literature values and our own studies on a separate cohort of TSM strips that showed them to have just minimal effects on isometric force (see *Isometric protocols* above). Also, these concentrations did not affect isotonic shortening to ACh, MLC_{20} phosphorylation, or activation state of p38 MAPK in the present study (see Results). After this equilibration period, the isotonic contraction protocol was repeated in the continued presence of inhibitor or vehicle (Figure 1). Muscle length changes during contractions before and after inhibitor treatment were expressed as %Lref. Near the end of the second contraction sequence, but before force fluctuations stopped, most tissues were flash-frozen in liquid nitrogen. Strips were then transferred to dry ice-chilled acetone (containing 5% trichloroacetic acid and 10 mM dithiothreitol), and stored at -80°C for protein extraction and Western blot analysis.

Jasplakinolide and U0126 combined studies. Previously, we showed that contractile actin polymerization plays a key role in regulating FFIR (16). This protocol was designed to test the hypothesis that MEK inhibition enhances FFIR by reducing actin filament stability. Tissues were equilibrated, Fmax determined, and the initial isotonic/force oscillation protocol was performed (as above). TSM strips were allowed to relax and then incubated for 1 hr in jasplakinolide (500 nM; EMD Biosciences, San Diego, CA), an agent that stabilizes actin filaments and promotes polymerization. While still in the presence of jasplakinolide, the contraction sequence was repeated. After completion of this second contraction sequence, tissues were allowed to relax to baseline in K-H containing 500 nM jasplakinolide. Once baseline relaxed tone was achieved, tissues were further incubated in 30 μM U0126 (in addition to 500 nM jasplakinolide) for 1 hr. A third combined contraction sequence was then performed in the presence of both U0126 and jasplakinolide. These tissues were designated CJU (control-jasplakinolide-jasplakinolide plus U0126) to depict the 3 isotonic/oscillation contraction sequences. Three control groups were also tested; CCC (control-vehicle-vehicle), CJJ (control-jasplakinolide-jasplakinolide), and CCU (control-vehicle-vehicle plus U0126). At the end of the third contraction sequence, but before force fluctuations had stopped, tissues were flash-frozen in liquid nitrogen and transferred to dry ice-chilled acetone (as above).

Western analysis of target protein phosphorylation. Proteins from U0126-, jasplakinolide-, and vehicle-treated muscles that had been frozen near the end of their respective contraction sequence were extracted as described previously (16, 30). All lanes in all gels were loaded with equal concentrations of total protein extracts. Denatured proteins were separated by SDS-polyacrylamide gel electrophoresis (Invitrogen, Carlsbad, CA) transferred to Immobilon-P

PVDF membranes, and probed for phosphorylated and total ERK1/2, h-caldesmon, MLC_{20}, p38 MAPK, and HSP27. Phosphorylated and total proteins were detected on separate PVDF membranes using SuperSignal West Pico (Thermo, Rockford, IL) chemiluminescent substrate, and blot intensities (volumes) were calculated using a BioRad densitometer (Hercules, CA) and software. Ratios of phosphorylated to total protein were expressed relative to data derived for vehicle-treated tissues on the same western blot.

All primary antibodies were raised in rabbits, and were from the following sources: phosphorylated (Ser^{789}) and non-phosphorylated h-caldesmon, Dr. Len Adam; HSP27 and phosphorylated MLC_{20}, Dr. W.T. Gerthoffer; phosphorylated HSP27 (Assay Designs, Ann Arbor, MI); MLC_{20} (Santa Cruz Biotechnology, Santa Cruz, CA); ERK1/2, Dr. Guy Drapeau; and phosphorylated and non-phosphorylated p38 MAPK and phosphorylated ERK1/2 (Cell Signaling, Danvers, MA).

Data Analysis. All data are expressed as mean ± SEM. All muscle lengths attained during agonist-elicited isotonic shortening and FFIR were expressed as %Lref. Differences between first and second isotonic/force oscillation sequence (i.e., before and after inhibitor or vehicle), or second and third contraction sequences for the jasplakinolide study, were expressed as ΔFFIR. Results from different groups were compared using ANOVA or Student's t-test for paired or unpaired data when appropriate. When ANOVA revealed a difference among means, data were further analyzed using Student-Newman-Keuls test for multiple comparisons. Significant differences were defined when $p < 0.05$.

RESULTS

MEK inhibition increases FFIR in a concentration-related fashion in ACh-contracted canine TSM. For each isotonic/oscillation contraction sequence, we calculated FFIR as the change in contracted muscle strip length that occurred during the 20 min period of oscillation (Figure 1); ΔFFIR was calculated from these values for each muscle strip. The effects on ΔFFIR of three concentrations of U0126, 3 μM, 15 μM, and 30 μM were compared to that of vehicle alone (Figure 2). U0126 increased ΔFFIR of ACh-contracted TSM strips in a concentration-dependent manner ($p < 0.001$). As in our previous studies (16), vehicle-treated tissues demonstrated reproducible FFIR post- vs. pre-treatment (i.e., ΔFFIR ~ zero). These data support the hypothesis that MEK regulates ΔFFIR in canine TSM.

MEK inhibition has no significant effect on isometric force generation or isotonic shortening in ACh-contracted canine TSM. The effects of 15 μM and 30 μM U0126 on isometric contraction of canine TSM were assessed. No significant shift in the concentration-response relationship to ACh was observed for either concentration of U0126, though strips treated with the higher concentration tended toward ($p = 0.269$) reduced force at 10^{-4} M ACh (Figure 3A). Isotonic shortening post-treatment was not different among tissues treated with 30 μM U0126 or vehicle (Figure 3B); as such, this parameter could not account for differences observed in ΔFFIR among groups.

MEK inhibition reduces caldesmon phosphorylation in ACh-contracted canine TSM. Increasing concentrations of U0126 progressively reduced h-caldesmon phosphorylation ($p=0.002$) (Figure 4A). As such, ΔFFIR (which progressively increased with increasing U0126 concentration,

Figure 2) varied inversely with the level of h-caldesmon phosphorylation (Figure 4B). As expected, U0126 treatment substantially reduced ERK1/2 phosphorylation at all concentrations studied (data not shown; $p < 0.001$). However, MEK inhibition had no significant effect on phosphorylation of MLC_{20}, p38 MAPK, or HSP27 (data not shown; $p > 0.25$ for each ANOVA).

MEK inhibition increases FFIR by a mechanism that does not involve loss of actin filament integrity. As we found previously (16), jasplakinolide alone (CJJ, n=3) had no effect on FFIR compared to control (CCC, n=4). Consistent with results from the 2-contraction protocol (Figure 1B), 30 μM U0126 significantly increased ΔFFIR in CCU (n=4) tissue strips ($p = 0.004$; ANOVA). CJU (n=3) strips were exposed to jasplakinolide during the second contraction sequence then jasplakinolide plus U0126 during the third. In these CJU strips, ΔFFIR remained equivalent to that observed in CCU tissues (p = NS). Jasplakinolide did not significantly alter the influence of U0126 on phosphorylation of either ERK1/2 or h-caldesmon (data not shown).

DISCUSSION

There is a growing body of evidence demonstrating that tidal breathing functionally opposes airway constriction induced by methacholine (7, 10, 13), and it seems very likely that FFIR of contracted airway smooth muscle may account for this anti-bronchoconstrictor effect. Therefore, it is of considerable interest to know what mechanisms determine FFIR and how smooth muscle might be manipulated to accentuate this salutary phenomenon. Previous studies clearly demonstrated that force fluctuations applied to isotonically contracted ASM result in considerable relengthening despite continued contractile stimulation (1, 4, 15, 16). Our present study extends those findings by demonstrating that: 1) FFIR can be augmented by inhibiting

MEK signaling pathway (Figures 1 and 2). 2) The effect of MEK inhibition on FFIR cannot be accounted for by changes in isometric force generation, isotonic shortening (Figure 3), reduced MLC_{20} phosphorylation, altered p38 MAPK activation, or actin filament dynamics, and so must depend on some other mechanism. 3) In contrast, the potentiation of FFIR caused by MEK inhibition varies inversely with concomitant inhibition of h-caldesmon phosphorylation (Figure 4B), suggesting that MEK regulates FFIR, at least in part, through its downstream target, h-caldesmon.

Muscarinic receptor activation involves a complex signaling cascade including activation of MEK and its downstream effectors (Figure 5). Several studies in a variety of species have demonstrated attenuation of contraction in smooth muscles by inhibition of the MEK signaling pathway (19, 31-34). Notably, D'Angelo and Adam (35) demonstrated in porcine carotid artery that inhibition of ERK activation using PD098059 caused attenuation of isometric force, with reductions in both MLC_{20} and h-caldesmon phosphorylation observed when tissues were activated by endothelin-1. Furthermore, Earley et al. showed that knocking down caldesmon expression reduced KCl-stimulated vascular smooth muscle contraction by 62% (36). Herein, we sought to assess the effects of MEK inhibition on FFIR in canine tracheal smooth muscle without reducing isometric force generation or isotonic shortening. Both 15 μM and 30 μM U0126 clearly had no effect on isotonic shortening (Figure 3B), and while the higher concentration of U0126 tended to reduce isometric force generation slightly, this agent had absolutely no effect on force generation when used at 15 μM (Figure 3A). Nonetheless, substantial and concentration-related augmentation of FFIR was observed. As the primary mechanistic intervention in these studies (i.e., U0126 treatment) directly modified MEK

activation, these significant changes indicate that MEK signaling negatively regulates FFIR through a mechanism that does not require alteration of more conventional measures of contraction, i.e., isometric force generation or isotonic shortening.

We evaluated several potential mechanisms by which MEK signaling might have exerted its regulatory influence on FFIR. Caldesmon is an actin-associated protein that appears to regulate force in vascular smooth muscle (35). Work from Adam's laboratory has shown that phosphorylation of h-caldesmon parallels isometric force production, and that ERK1/2 are "physiologically relevant" caldesmon kinases (35). When caldesmon becomes phosphorylated on Ser^{789} by active ERK1/2, actomyosin interaction is disinhibited (24-27). In our study, U0126 significantly reduced ERK1/2 phosphorylation and, to a lesser extent, caldesmon phosphorylation, and we found an inverse relationship between ΔFFIR and level of caldesmon phosphorylation at Ser^{789} (Figure 4B). Thus, our results suggest a potential role for h-caldesmon phosphorylation – at least on Ser^{789} – in regulating the magnitude of FFIR. Despite inhibition of ERK 1/2 activation by U0126 treatment, partial caldesmon phosphorylation still occurred. Consistent with these findings, others have shown that inhibition of MEK signaling reduces but does not abolish caldesmon phosphorylation (37, 38). In addition, U0126 at the higher concentrations showed a disproportionate increase in FFIR in relation to the more modest decrease in caldesmon phosphorylation. This suggests that MEK inhibition acts through more than one mechanism to influence FFIR and perhaps additional inhibition of other purported caldesmon kinases, such as $p34^{cdc2}$ (39), p21 activated kinase (40, 41), casein kinase 2 (42), or CaM kinase II (43), might enhance FFIR even more dramatically.

We also explored several other potential mechanisms by which MEK inhibition might contribute to augmenting FFIR. MEK signaling can catalyze the downstream phosphorylation of tropomyosin (44), an actin side-binding protein that stabilizes actin filaments. Phosphorylated tropomyosin binds with increased affinity to actin filaments. Therefore, we hypothesized that MEK signaling might lead to stabilized actin filaments. Since we previously showed that stabilization of actin filaments with jasplakinolide blocks latrunculin B-induced increases in FFIR (16), we tested this hypothesis by determining whether jasplakinolide could also block MEK inhibition-induced increases in FFIR. As reported in the results, jasplakinolide pretreatment could not prevent the effect of U0126 on ΔFFIR. Thus, it appears that MEK signaling reduces FFIR through a mechanism that does not involve loss of actin filament integrity. However, it remains conceivable that interaction between actin filaments and the cell membrane at focal adhesions might be involved.

Interestingly, there was no significant change in MLC_{20} phosphorylation with MEK inhibition. Previously, we had reasoned that increased actomyosin crossbridge cycling might reduce the net effect of stretch on contracted airway smooth muscle (4, 8, 15, 45, 46). In this study, MLC_{20} phosphorylation was not affected by U0126 treatment, and tissues treated with or without U0126 shortened similarly (Figure 3B). Since MLC_{20} phosphorylation is a key determinant of actomyosin crossbridge cycling rate, it seems likely that MEK inhibition had little influence on actomyosin ATPase activity. Thus, the MEK pathway regulates FFIR in canine TSM by a mechanism other than through changing MLC_{20} phosphorylation (or, presumably, actomyosin crossbridge cycling rate). However, it is conceivable that actin-myosin binding per se is impaired

with reduced h-caldesmon phosphorylation (40, 47, 48), which may explain why inhibition of MEK and thus reduced h-caldesmon phosphorylation augments FFIR in our tissues.

Finally, Lakser et al (15) had previously shown that p38 MAPK activation inhibits FFIR in contracted bovine TSM. Other studies suggest that crosstalk between MEK/ERK1/2 and p38 MAPK signaling pathways can occur (49-52). However, since U0126 did not affect phosphorylation levels of p38 MAPK or HSP27 in our studies, MEK inhibition apparently did not exert its influence on FFIR by altering p38 MAPK signaling.

To our knowledge there are no reports of increased MEK activation in asthmatics vs. non-asthmatics; however, Burgess et al. (53) reported an increase in ERK phosphorylation in asthmatic human ASM cells in the presence of low concentrations of FBS. Furthermore, Duan et al. (54) showed that U0126 significantly reduced ovalbumin-induced airway hyperresponsiveness to methacholine in their mouse asthma model. Interestingly, ERK phosphorylation was also increased in the ovalbumin-challenged mice compared to the naïve mice suggesting a potential role for the MEK/ERK signaling pathway in allergic asthma models.

In conclusion, this study shows that the MEK signaling pathway regulates the magnitude of force fluctuation-induced relengthening of contracted airway smooth muscle, through a mechanism that in part involves h-caldesmon, but does not appear to depend upon changes in MLC_{20} phosphorylation, p38 MAPK signaling, or actin filament integrity. Since FFIR may account, at least in part, for the functional antagonism of bronchoconstriction by tidal breathing, our results have potential implications for the effects of force oscillations imparted by breathing on airflow

obstruction during bronchoconstrictor stimulation. Because FFIR is physiologically regulated (as evidenced by our ability to influence FFIR by manipulation of MEK activity), it seems conceivable that therapeutic intervention to increase FFIR in asthma may be beneficial.

REFERENCES

1. Oliver MN, Fabry B, Marinkovic A, Mijailovich SM, Butler JP, Fredberg JJ. Airway hyperresponsiveness, remodeling, and smooth muscle mass: right answer, wrong reason? Am J Respir Cell Mol Biol. 2007 Sep;37(3):264-72.

2. Fredberg JJ. Bronchospasm and its biophysical basis in airway smooth muscle. Respir Res. 2004;5:2.

3. Fredberg JJ, Inouye D, Miller B, Nathan M, Jafari S, Raboudi SH, et al. Airway smooth muscle, tidal stretches, and dynamically determined contractile states. Am J Respir Crit Care Med. 1997 Dec;156(6):1752-9.

4. Fredberg JJ, Inouye DS, Mijailovich SM, Butler JP. Perturbed equilibrium of myosin binding in airway smooth muscle and its implications in bronchospasm. Am J Respir Crit Care Med. 1999 Mar;159(3):959-67.

5. Gerthoffer WT, Gunst SJ. Invited review: focal adhesion and small heat shock proteins in the regulation of actin remodeling and contractility in smooth muscle. J Appl Physiol. 2001 Aug;91(2):963-72.

6. Gunst SJ, Fredberg JJ. The first three minutes: smooth muscle contraction, cytoskeletal events, and soft glasses. J Appl Physiol. 2003 Jul;95(1):413-25.

7. Gunst SJ, Shen X, Ramchandani R, Tepper RS. Bronchoprotective and bronchodilatory effects of deep inspiration in rabbits subjected to bronchial challenge. J Appl Physiol. 2001 Dec;91(6):2511-6.

8. Latourelle J, Fabry B, Fredberg JJ. Dynamic equilibration of airway smooth muscle contraction during physiological loading. J Appl Physiol. 2002 Feb;92(2):771-9.

9. Salerno FG, Shinozuka N, Fredberg JJ, Ludwig MS. Tidal volume amplitude affects the degree of induced bronchoconstriction in dogs. J Appl Physiol. 1999 Nov;87(5):1674-7.

10. Shen X, Gunst SJ, Tepper RS. Effect of tidal volume and frequency on airway responsiveness in mechanically ventilated rabbits. J Appl Physiol. 1997 Oct;83(4):1202-8.

11. Freedman S, Lane R, Gillett MK, Guz A. Abolition of methacholine induced bronchoconstriction by the hyperventilation of exercise or volition. Thorax. 1988 Aug;43(8):631-6.

12. Gump A, Haughney L, Fredberg J. Relaxation of activated airway smooth muscle: relative potency of isoproterenol vs. tidal stretch. J Appl Physiol. 2001 Jun;90(6):2306-10.

13. Murphy TM, Ray DW, Alger LE, Phillips IJ, Roach JC, Leff AR, et al. Ontogeny of dry gas hyperpnea-induced bronchoconstriction in guinea pigs. J Appl Physiol. 1994 Mar;76(3):1150-5.

14. Skloot G, Permutt S, Togias A. Airway hyperresponsiveness in asthma: a problem of limited smooth muscle relaxation with inspiration. J Clin Invest. 1995 Nov;96(5):2393-403.

15. Lakser OJ, Lindeman RP, Fredberg JJ. Inhibition of the p38 MAP kinase pathway destabilizes smooth muscle length during physiological loading. Am J Physiol Lung Cell Mol Physiol. 2002 May;282(5):L1117-21.

16. Dowell ML, Lakser OJ, Gerthoffer WT, Fredberg JJ, Stelmack GL, Halayko AJ, et al. Latrunculin B increases force fluctuation-induced relengthening of ACh-contracted, isotonically shortened canine tracheal smooth muscle. J Appl Physiol. 2005 Feb;98(2):489-97.

17. Yamboliev IA, Hedges JC, Mutnick JL, Adam LP, Gerthoffer WT. Evidence for modulation of smooth muscle force by the p38 MAP kinase/HSP27 pathway. Am J Physiol Heart Circ Physiol. 2000 Jun;278(6):H1899-907.

18. Cao W, Sohn UD, Bitar KN, Behar J, Biancani P, Harnett KM. MAPK mediates PKC-dependent contraction of cat esophageal and lower esophageal sphincter circular smooth muscle. Am J Physiol Gastrointest Liver Physiol. 2003 Jul;285(1):G86-95.

19. Gerthoffer WT, Yamboliev IA, Shearer M, Pohl J, Haynes R, Dang S, et al. Activation of MAP kinases and phosphorylation of caldesmon in canine colonic smooth muscle. J Physiol. 1996 Sep 15;495 (Pt 3):597-609.

20. Kim HR, Hai CM. Mechanisms of mechanical strain memory in airway smooth muscle. Can J Physiol Pharmacol. 2005 Oct;83(10):811-5.

21. Gerthoffer WT. Signal-transduction pathways that regulate visceral smooth muscle function. III. Coupling of muscarinic receptors to signaling kinases and effector proteins in gastrointestinal smooth muscles. Am J Physiol Gastrointest Liver Physiol. 2005 May;288(5):G849-53.

22. Deng JT, Van Lierop JE, Sutherland C, Walsh MP. Ca2+-independent smooth muscle contraction. a novel function for integrin-linked kinase. J Biol Chem. 2001 May 11;276(19):16365-73.

23. Harnett KM, Biancani P. Calcium-dependent and calcium-independent contractions in smooth muscles. Am J Med. 2003 Aug 18;115 Suppl 3A:24S-30S.

24. Cook AK, Carty M, Singer CA, Yamboliev IA, Gerthoffer WT. Coupling of M(2) muscarinic receptors to ERK MAP kinases and caldesmon phosphorylation in colonic smooth muscle. Am J Physiol Gastrointest Liver Physiol. 2000 Mar;278(3):G429-37.

25. D'Angelo G, Graceffa P, Wang CA, Wrangle J, Adam LP. Mammal-specific, ERK-dependent, caldesmon phosphorylation in smooth muscle. Quantitation using novel anti-phosphopeptide antibodies. J Biol Chem. 1999 Oct 15;274(42):30115-21.

26. Hedges JC, Oxhorn BC, Carty M, Adam LP, Yamboliev IA, Gerthoffer WT. Phosphorylation of caldesmon by ERK MAP kinases in smooth muscle. Am J Physiol Cell Physiol. 2000 Apr;278(4):C718-26.

27. Li Y, Je HD, Malek S, Morgan KG. ERK1/2-mediated phosphorylation of myometrial caldesmon during pregnancy and labor. Am J Physiol Regul Integr Comp Physiol. 2003 Jan;284(1):R192-9.

28. Mitchell RW, Antonissen LA, Kepron W, Kroeger EA, Stephens NL. Effect of atropine on the hyperresponsiveness of ragweed-sensitized canine tracheal smooth muscle. J Pharmacol Exp Ther. 1986 Mar;236(3):803-9.

29. Lakser OJ, Dowell ML, Hoyte FL, Chen B, Lavoie TL, Ferreira C, et al. Steroids augment relengthening of contracted airway smooth muscle: potential additional mechanism of benefit in asthma. Eur Respir J. 2008 Nov;32(5):1224-30.

30. Mitchell RW, Halayko AJ, Kahraman S, Solway J, Wylam ME. Selective restoration of calcium coupling to muscarinic M(3) receptors in contractile cultured airway myocytes. Am J Physiol Lung Cell Mol Physiol. 2000 May;278(5):L1091-100.

31. Lagaud GJ, Lam E, Lui A, van Breemen C, Laher I. Nonspecific inhibition of myogenic tone by PD98059, a MEK1 inhibitor, in rat middle cerebral arteries. Biochem Biophys Res Commun. 1999 Apr 13;257(2):523-7.

32. Pearce WJ, Williams JM, Chang MM, Gerthoffer WT. ERK inhibition attenuates 5-HT-induced contractions in fetal and adult ovine carotid arteries. Arch Physiol Biochem. 2003 Feb;111(1):36-44.

33. Xiao D, Pearce WJ, Longo LD, Zhang L. ERK-mediated uterine artery contraction: role of thick and thin filament regulatory pathways. Am J Physiol Heart Circ Physiol. 2004 May;286(5):H1615-22.

34. Xiao D, Zhang L. ERK MAP kinases regulate smooth muscle contraction in ovine uterine artery: effect of pregnancy. Am J Physiol Heart Circ Physiol. 2002 Jan;282(1):H292-300.

35. D'Angelo G, Adam LP. Inhibition of ERK attenuates force development by lowering myosin light chain phosphorylation. Am J Physiol Heart Circ Physiol. 2002 Feb;282(2):H602-10.

36. Earley JJ, Su X, Moreland RS. Caldesmon inhibits active crossbridges in unstimulated vascular smooth muscle: an antisense oligodeoxynucleotide approach. Circ Res. 1998 Sep 21;83(6):661-7.

37. Gorenne I, Su X, Moreland RS. Caldesmon phosphorylation is catalyzed by two kinases in permeabilized and intact vascular smooth muscle. J Cell Physiol. 2004 Mar;198(3):461-9.

38. Krymsky MA, Chibalina MV, Shirinsky VP, Marston SB, Vorotnikov AV. Evidence against the regulation of caldesmon inhibitory activity by p42/p44erk mitogen-activated protein kinase in vitro and demonstration of another caldesmon kinase in intact gizzard smooth muscle. FEBS Lett. 1999 Jun 11;452(3):254-8.

39. Mak AS, Carpenter M, Smillie LB, Wang JH. Phosphorylation of caldesmon by p34cdc2 kinase. Identification of phosphorylation sites. J Biol Chem. 1991 Oct 25;266(30):19971-5.

40. Foster DB, Shen LH, Kelly J, Thibault P, Van Eyk JE, Mak AS. Phosphorylation of caldesmon by p21-activated kinase. Implications for the Ca(2+) sensitivity of smooth muscle contraction. J Biol Chem. 2000 Jan 21;275(3):1959-65.

41. McFawn PK, Shen L, Vincent SG, Mak A, Van Eyk JE, Fisher JT. Calcium-independent contraction and sensitization of airway smooth muscle by p21-activated protein kinase. Am J Physiol Lung Cell Mol Physiol. 2003 May;284(5):L863-70.

42. Vorotnikov AV, Gusev NB, Hua S, Collins JH, Redwood CS, Marston SB. Identification of casein kinase II as a major endogeneous caldesmon kinase in sheep aorta smooth muscle. FEBS Lett. 1993 Nov 8;334(1):18-22.

43. Ikebe M, Reardon S. Phosphorylation of smooth myosin light chain kinase by smooth muscle Ca2+/calmodulin-dependent multifunctional protein kinase. J Biol Chem. 1990 Jun 5;265(16):8975-8.

44. Houle F, Rousseau S, Morrice N, Luc M, Mongrain S, Turner CE, et al. Extracellular signal-regulated kinase mediates phosphorylation of tropomyosin-1 to promote cytoskeleton remodeling in response to oxidative stress: impact on membrane blebbing. Mol Biol Cell. 2003 Apr;14(4):1418-32.

45. Dulin NO, Fernandes DJ, Dowell M, Bellam S, McConville J, Lakser O, et al. What evidence implicates airway smooth muscle in the cause of BHR? Clin Rev Allergy Immunol. 2003 Feb;24(1):73-84.

46. Solway J, Bellam S, Dowell M, Camoretti-Mercado B, Dulin N, Fernandes D, et al. Actin dynamics: a potential integrator of smooth muscle (Dys-)function and contractile apparatus gene expression in asthma. Parker B. Francis lecture. Chest. 2003 Mar;123(3 Suppl):392S-8S.

47. Huang R, Li L, Guo H, Wang CL. Caldesmon binding to actin is regulated by calmodulin and phosphorylation via different mechanisms. Biochemistry. 2003 Mar 11;42(9):2513-23.

48. Kulikova N, Avrova SV, Borovikov YS. Caldesmon inhibits the rotation of smooth actin subdomain-1 and alters its mobility during the ATP hydrolysis cycle. Biochem Biophys Res Commun. 2009 Dec 4;390(1):125-9.

49. Houliston RA, Pearson JD, Wheeler-Jones CP. Agonist-specific cross talk between ERKs and p38(mapk) regulates PGI(2) synthesis in endothelium. Am J Physiol Cell Physiol. 2001 Oct;281(4):C1266-76.

50. Kurosawa M, Numazawa S, Tani Y, Yoshida T. ERK signaling mediates the induction of inflammatory cytokines by bufalin in human monocytic cells. Am J Physiol Cell Physiol. 2000 Mar;278(3):C500-8.

51. Liu Q, Hofmann PA. Protein phosphatase 2A-mediated cross-talk between p38 MAPK and ERK in apoptosis of cardiac myocytes. Am J Physiol Heart Circ Physiol. 2004 Jun;286(6):H2204-12.

52. Xiao YQ, Malcolm K, Worthen GS, Gardai S, Schiemann WP, Fadok VA, et al. Cross-talk between ERK and p38 MAPK mediates selective suppression of pro-inflammatory cytokines by transforming growth factor-beta. J Biol Chem. 2002 Apr 26;277(17):14884-93.

53. Burgess JK, Lee JH, Ge Q, Ramsay EE, Poniris MH, Parmentier J, et al. Dual ERK and phosphatidylinositol 3-kinase pathways control airway smooth muscle proliferation: differences in asthma. J Cell Physiol. 2008 Sep;216(3):673-9.

54. Duan W, Chan JH, Wong CH, Leung BP, Wong WS. Anti-inflammatory effects of mitogen-activated protein kinase kinase inhibitor U0126 in an asthma mouse model. J Immunol. 2004 Jun 1;172(11):7053-9.

FIGURE LEGENDS

Figure 1: *Experimental protocol*. In these representative tracings, tracheal smooth muscle strips were exposed to U0126 or vehicle (control) for 45 minutes after which the oscillation protocol was then repeated. Differences in force fluctuation-induced relengthening (ΔFFIR) post- vs. pre-treatment were compared. For the vehicle-treated (control) muscle strip (panel A), there was no appreciable difference in FFIR comparing post- to pre-treatment. MEK inhibition with U0126 (panel B) significantly increased ΔFFIR relative to vehicle treated control strips.

Figure 2: *ΔFFIR correlates with U0126 concentration in canine tracheal smooth muscle (TSM) strips contracted with ACh.* To determine whether ΔFFIR correlated with the concentration of MEK inhibitor, the effect of varying U0126 concentration was investigated. Three concentrations of U0126 were used; 3 μM (n=6), 15 μM (n=6), and 30 μM (n=6) and the ΔFFIR were compared to TSM strips that received vehicle alone (n=14). These data show that MEK inhibition modulates FFIR in a concentration-dependent manner ($p<0.001$; ANOVA). (* denotes significant difference vs. the no drug treatment group. # denotes significant difference vs. 15 μM U0126, 3 μM U0126, and the no drug treatment groups.) Values are means ± SE.

Figure 3: *Effect of MEK inhibition on isometric responsiveness and isotonic shortening in ACh-contracted canine tracheal smooth muscle (TSM) strips*. **A**: U0126 at 15 μM (n=3) and 30 μM (n=5) had no significant effect on isometric responsiveness compared to control strips (n=4) ($p= 0.486$; ANOVA) **B**: Although 30 μM U0126 (n=6) treatment resulted in a substantial increase in ΔFFIR compared to control (n=14), it did not affect isotonic shortening of the TSM strips post treatment ($p= 0.951$; Student's t-test). Values are means ± SE.

Figure 4: *Effect of MEK inhibition on caldesmon phosphorylation in canine tracheal smooth muscle (TSM) strips*. **A:** Three concentrations of U0126 were used: 3 μM (n= 6), 15 μM (n= 5), and 30 μM (n= 6). Caldesmon phosphorylation levels were compared to TSM strips that received vehicle alone (n= 10). Caldesmon demonstrated reduced phosphorylation after treatment with 15 μM and 30 μM U0126 compared to both vehicle-treated and 3 μM strips ($p= 0.002$; ANOVA). Also included in panel A is a representative Western blot of control and U0126 treated tissues. **B:** ΔFFIR varies inversely with caldesmon phosphorylation in strips contracted with ACh in the presence of U0126. These data are reproduced from Figures 2 and 4A. (* denotes significant difference vs. the no drug treatment group, ** significant vs. the no drug treatment and 3 μM U0126, and # significant vs. the 15 μM U0126, 3 μM U0126, and no drug treatment groups.) Values are means ± SE.

Figure 5: *Schematic model of signaling pathways involved in smooth muscle contraction*. Acetylcholine (ACh) activates G protein-coupled muscarinic receptors (M2R and M3R), resulting in the activation of several signaling cascades. M2R activates Raf/MEK signaling that in turn activates extracellular signal-regulated kinases (ERK) 1/2 and their downstream

regulators of contraction, including h-caldesmon. Through activation of myosin light chain kinase (MLCK) and ERK1/2, intracellular Ca^{2+} and ILK (integrin-linked kinase) promote phosphorylation of myosin light chain 20 (P-MLC_{20}). Only a few of the likely effector molecules involved in this pathway are depicted. PKC, protein kinase C; DAG, diacylglycerol; IP3, inositol 1,4,5-triphosphate; Ca^{2+}-CaM, Ca^{2+}-calmodulin; MEK, MAPK kinase; PI 3-K, phosphatidylinositol 3-kinase; HSP 27, heat shock protein 27.

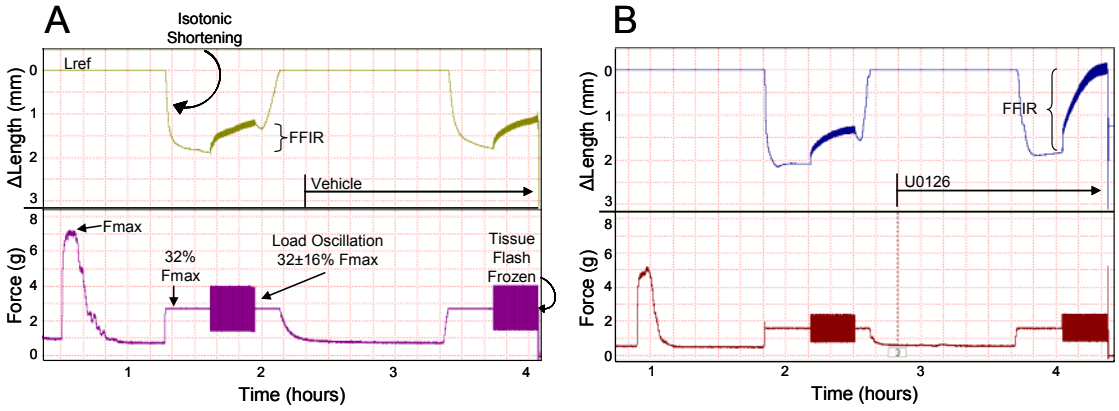

Figure 1

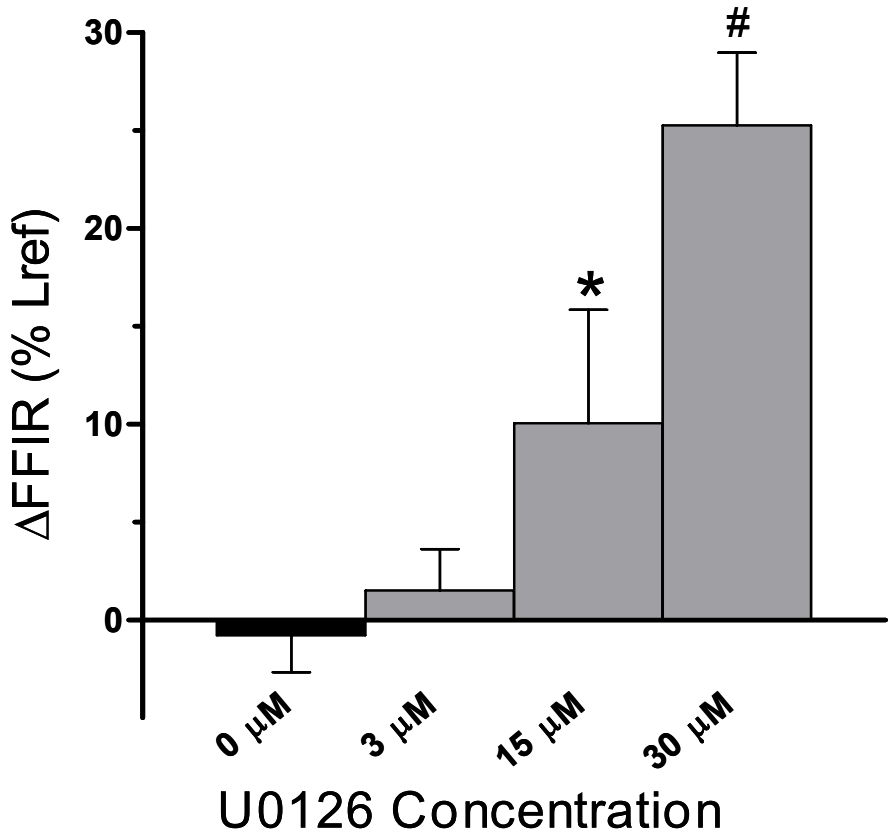

Figure 2

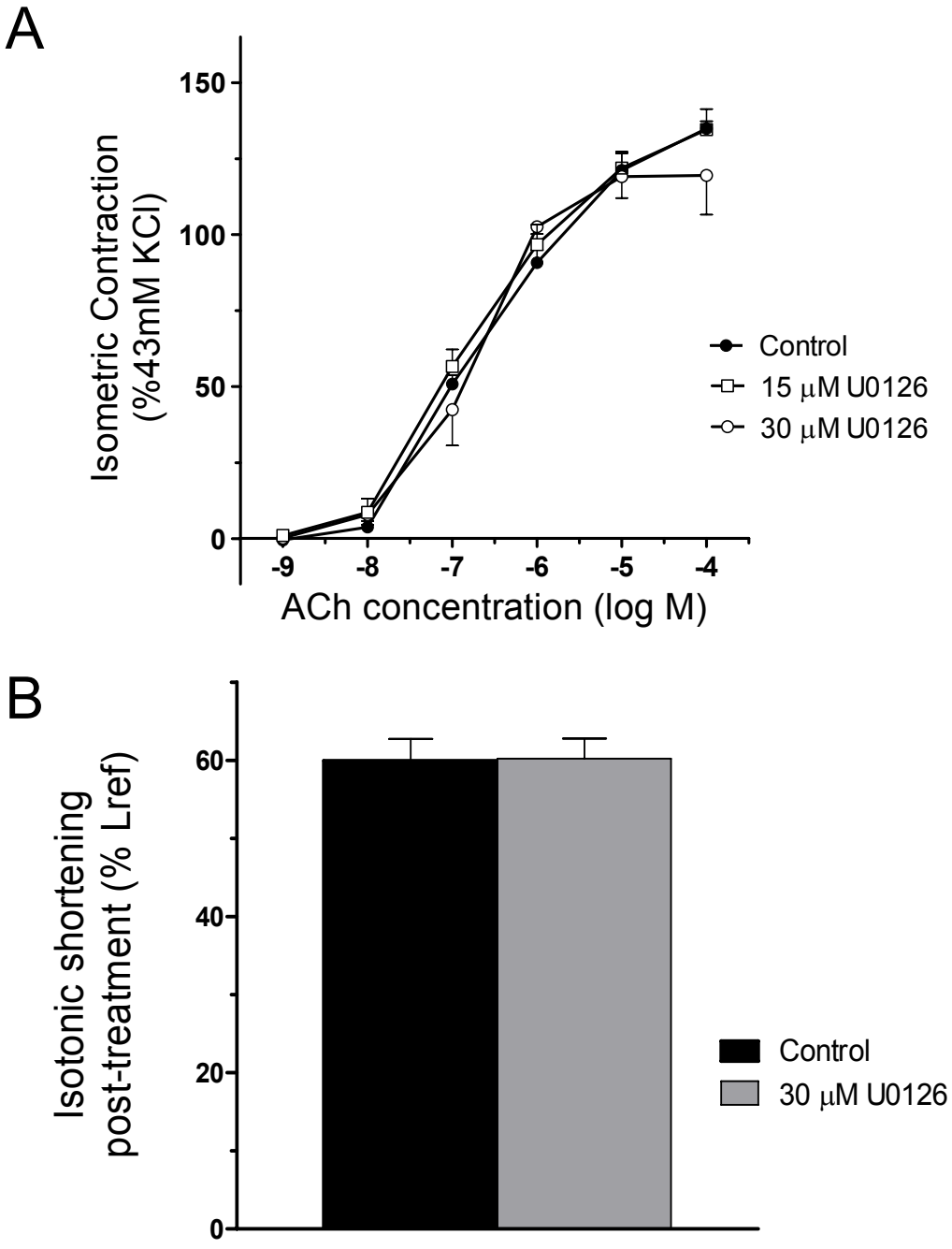
A
Isometric Contraction
(%43mM KCl)
150
100
50
0
-9
-8
-7
-6
-5
-4
ACh concentration (log M)
Control
15 μM U0126
30 μM U0126
B
Isotonic shortening
post-treatment (% Lref)
60
40
20
0
Control
30 μM U0126

Figure 3

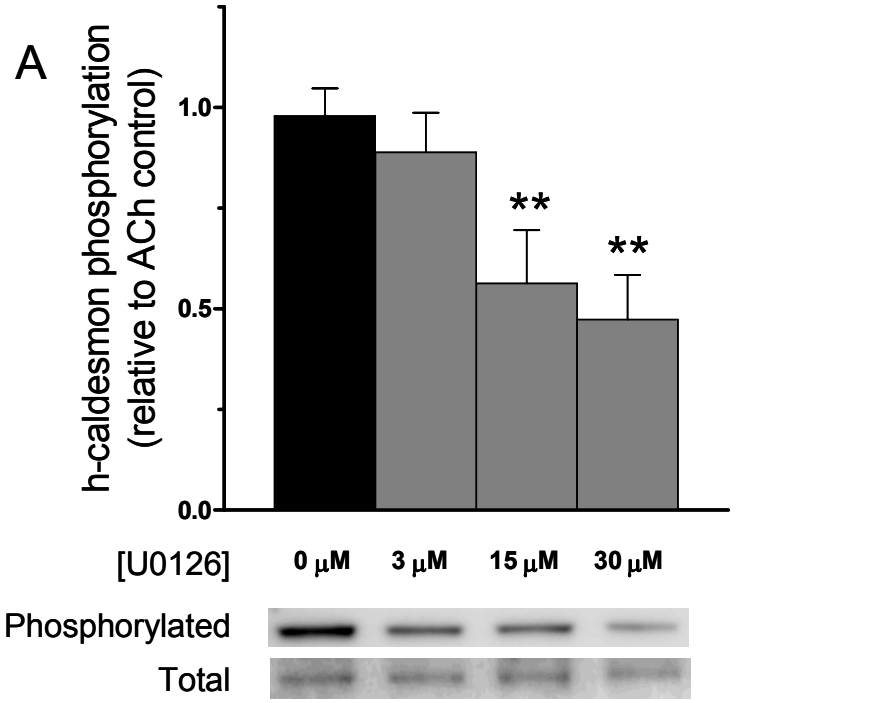
A
h-caldesmon phosphorylation
(relative to ACh control)
1.0
0.5
0.0
**
**
[U0126]
0 μM
3 μM
15 μM
30 μM
Phosphorylated
Total

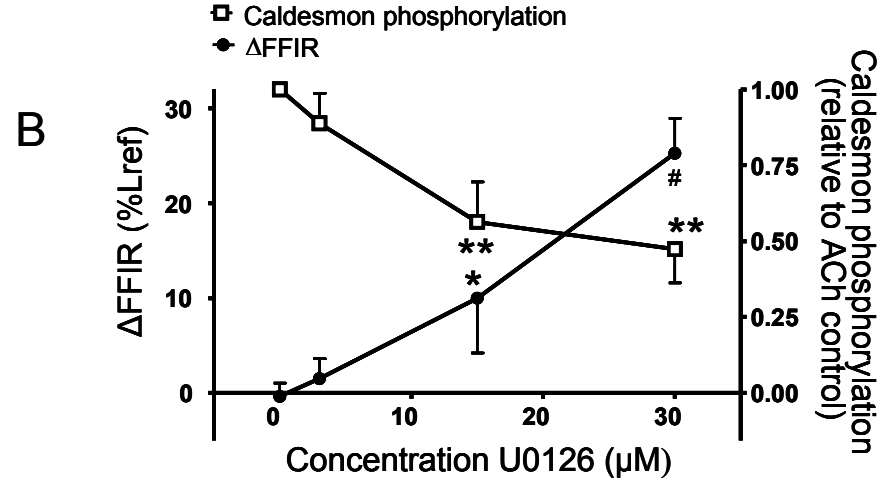
Caldesmon phosphorylation
ΔFFIR
B
ΔFFIR (%Lref)
30
20
10
0
1.00
0.75
0.50
0.25
0.00
Caldesmon phosphorylation
(relative to ACh control)
**
*
#
**
0
10
20
30
Concentration U0126 (μM)

Figure 4

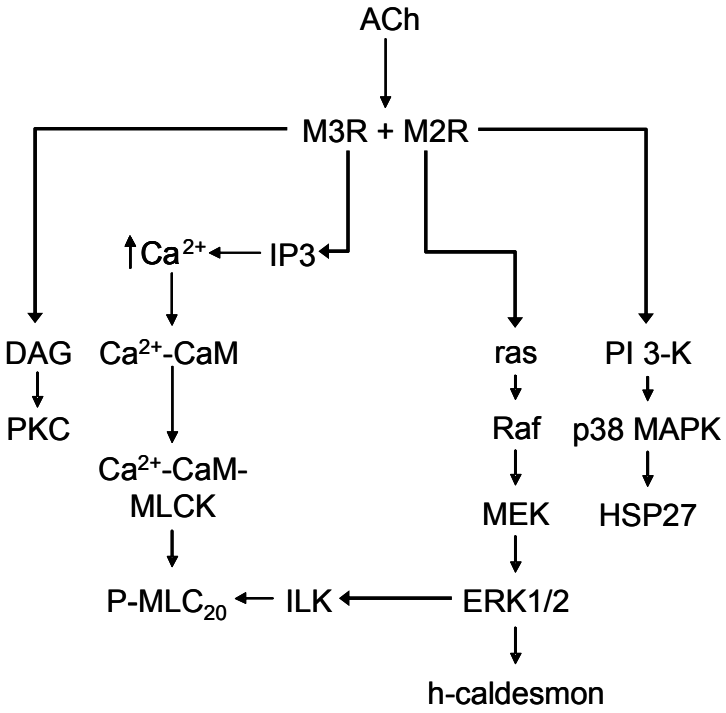
ACh
M3R + M2R
↑Ca2+
IP3
DAG
Ca2+-CaM
ras
PI 3-K
PKC
Raf
p38 MAPK
Ca2+-CaM-
MLCK
MEK
HSP27
P-MLC20
ILK
ERK1/2
h-caldesmon

Figure 5